International Journal of High Speed Electronics and Systems
Vol. 20, No. 1 (2011) 143–152

DOI: 10.1142/S0129156411006477

World Scientific
www.worldscientific.com

ELECTRON HEATING IN QUANTUM-DOT STRUCTURES WITH COLLECTIVE POTENTIAL BARRIERS

L.H. CHIEN

EE Department, University at Buffalo, The State University of New York, 321 Bonner Hall, Buffalo, NY 14260, USA
lchien2@buffalo.edu

A. SERGEEV

SUNY Research Foundation, University at Buffalo, The State University of New York, 320 Bonner Hall, Buffalo, NY 14260, USA
asergeev@eng.buffalo.edu

N. VAGIDOV

EE Department, University at Buffalo, The State University of New York, 312 Bonner Hall, Buffalo, NY 14260, USA
nizami@buffalo.edu

V. MITIN

EE Department, University at Buffalo, The State University of New York, 312 Bonner Hall, Buffalo, NY 14260, USA
vmitin@buffalo.edu

S. BIRNER

Physics Department, Technische Iniversitat Munchen, Am Coulombwall 3, D-85748 Garching, Germany
stefan.birner@wsi.tum.de

Here we report our research on quantum-dot structures with collective barriers surrounding groups of quantum dots (planes, clusters etc) and preventing photoelectron capture. Employing Monte-Carlo simulations, we investigate photoelectron kinetics and calculate the photoelectron lifetime as a function of geometrical parameters of the structures, dot occupation, and electric field. Results of our simulations demonstrate that the capture processes are substantially suppressed by the potential barriers and enhanced in strong electric fields. Detailed analysis shows that the effects of the electric field can be explained by electron heating, i.e. field effects become significant, when the shift of the electron temperature due to electron heating reaches the barrier height. Optimized photoelectron kinetics in quantum-dot structures with collective barriers allows for significant improvements in the photoconductive gain, detectivity, and responsivity of photodetectors based on these structures.

Keywords: quantum-dot photodetector; potential barriers; photoelectron lifetime; capture; gain.

1. Introduction

Adequate understanding of photoelectron kinetics in nanostructures is critically important for attainment of high performance in room-temperature semiconductor optoelectronic devices, such as mid- and far-infrared detectors, solar cells, etc.[1-6] During many years quantum-dot nanostructures were considered as a promising candidate for improving the room-temperature operation due to expected slow relaxation between discrete QD levels. These expectations were based on the "phonon bottleneck" concept, which assumes that the phonon-assisted bound-to-bound transitions are prohibited, unless the energy between two discrete levels matches the phonon energy.[7] According to this concept, the intrinsic electron relaxation in QDs was anticipated to be significantly slower than that in 2D and 3D structures. However, the phonon bottleneck model completely ignores modification of electron states due to interaction effects, e.g. due to a finite width of electron energy levels.

Recent investigations[1] unambiguously demonstrated that the actual intra-dot kinetics is completely opposite to what can be expected for weakly interacting electrons and phonons. In reality, strong coupling between electrons and longitudinal optical (LO) phonons leads to formation of the polaron states, which decay due to the interaction of LO phonons with acoustical phonons. Such kinetics results in strong energy and temperature dependences of the electron relaxation. At helium temperature, long relaxation time (~ 1.5 ns) was observed for the level separation of 14 meV (3.4 THz).[1] However, the relaxation time decreases to ~ 2 ps for the 30 meV transition. The relaxation time also drastically decreases, if temperature increases. For example, for 14 meV transition, the relaxation time was reduced from 1.5 ns at 10 K to 560 ps at 30 K, and further to 260 ps at 50 K. At room temperatures the polaron decay time is observed in the range of 2 – 30 ps, depending on the electron energy.[1] After numerous experiments[1,8-10] with various QD structures, no true phonon bottleneck has been found. Thus, the intra-dot electron kinetics at room temperatures turns out to be very fast and practically unmanageable.

In our previous publications[11-15] we proposed to manage inter-dot kinetics and suppress photocarrier capture processes by means of the barriers, which are formed by electrons bounded in quantum dots and ionized impurities in the depletion region. These potential barriers separate the conducting electron states from the localized intra-dot states and prevent photoelectron capture into the dots. Modern technologies provide many possibilities to fabricate QD infrared photodetectors (QDIPs) with local and collective potential barriers. The local potential barrier around a single dot can be formed by homogeneous doping of the interdot space. To suppress electron capture process, the barrier height should be at least two - three times larger than kT. Therefore, at room temperatures, the local barriers should be ~ 0.1 eV and quantum dots should comprise at least ten electrons. This requires large size dots and very high level of doping.

At the same time, significant potential barriers that effectively separate conducting and localized states can be created by groups of quantum dots (dot clusters, rows etc).[16] Such collective barriers divide the groups of quantum dots from high-mobility conducting channels. In this work we report results of our modeling of photoelectron kinetics and transport in QD structure with collective potential barriers.

2. Nanostructures with Collective Barriers

The QD structures with collective potential barriers provide new possibilities to suppress capture processes and control photocarrier kinetics. Fig. 1.a shows the QD structure with the lateral transport along high-mobility heterointerfaces, Fig. 1.b demonstrates the QD structure with vertically correlated dot clusters (VCDC) and the vertical transport through inter-cluster areas. In a QD structure with the lateral transport (Fig. 1.a) the potential barriers are formed by charged QD planes and charged planes of dopants. In VCDC structures (Fig. 1.b) the barriers are created by charged dot clusters.

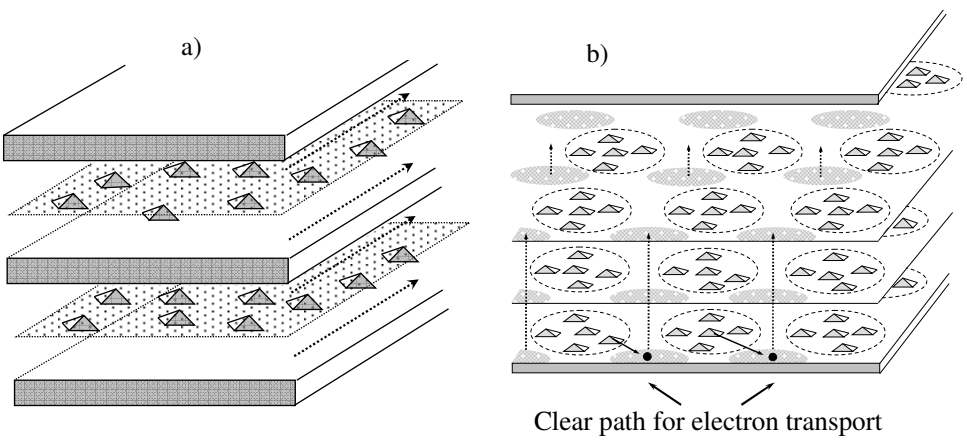

Fig. 1. (a). Schematic view of QD structures with collective potential barriers, which separate QD areas from the areas transmitting the photocurrent: (a) Structure with lateral transport (dashed arrows) along 2D heterointerfaces, (b) Structure with vertically correlated QD clusters and vertical transport in the inter-cluster areas. QDs are separated from conducting channels by potential barriers, which suppress photoelectron capture into QDs.

For example, the photodetector with the lateral transport (Fig. 1.a) may be realized on the basis of modulation-doped AlGaAs/GaAs structures with self-assembled InAs dots. QD planes are imbedded in the middle of GaAs quantum well with a thickness $2d$. AlGaAs layers are doped to supply free carriers. This lateral QDIP conducts photocurrent through high-mobility two-dimensional channels along the heterointerfaces of AlGaAs/GaAs. The potential barriers are formed by the ionized dopants in AlGaAs and the charges in QDs and have the form of $V_m = e^2 N_d^{(2)} nd/(2\varepsilon\varepsilon_0)$, where $N_d^{(2)}$ is the dot concentration in QD planes and n is the average occupation in the dots.

The detector based on the structures with the vertically correlated dot clusters is shown in Fig. 1.b. Positions of the dot clusters are correlated in the vertical direction, which is the direction of photocurrent. The collective barriers around dot clusters are created by charged dots and ionized dopants. This structure has the advantage of the vertical QDIP, which utilizes the mature and well-established technology for Ohmic contacts. In both structures, the electrons can be directly excited to the conducting states or excited to the

quasi-localized high-energy states and then emitted to the conducting states via thermoexcitation, tunneling, or photon-assisted tunneling. In VCDC structures the photoelectrons move in the areas between dot clusters through the high-mobility channels. If the radius of the cluster, b, exceeds the distance between dot layers, c, the potential barrier around dot clusters has a logarithmic form of $V_m = e^2Nn/(2\pi\varepsilon\varepsilon_0 c)\ln(w/b)$, where N is the number of dots in the cluster, n is the average number of carriers per dot, and $2w$ is the distance between the centers of two neighboring clusters, so the dot cluster concentration is $N_c = N_d^{(2)}/N$, where $N_d^{(2)}$ is the dot concentration in the QD planes.

The self-consistent 3D-simulations of VCDC structures using nextnano3 software developed at the Walter Schottky Institut,[17] gives the spatial distribution of potential profile with barriers surronding individual QDs as well as around the cluster of QDs (see Fig. 2. Cluster consisting of 9 InAs QDs in GaAs matrix is shown encircled).

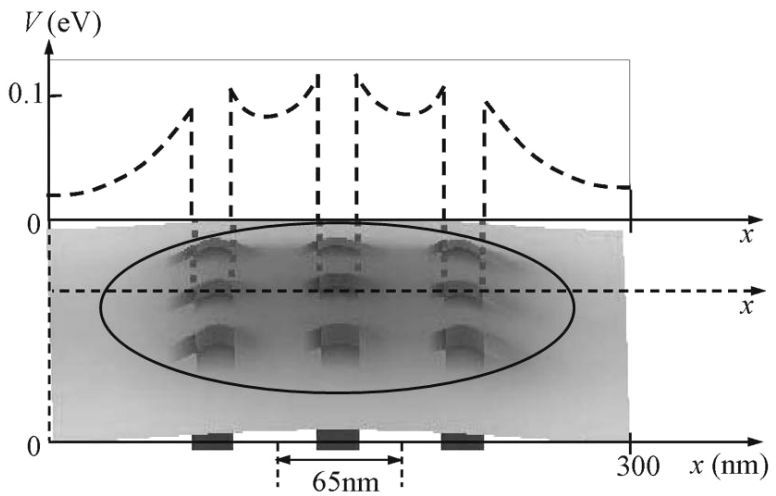

Fig. 2. The potential profile of the layer of VCDC structure with 9 QDs per cluster. The dimensions of InAs QDs in GaAs matrix are 20×20×10 nm^3, QD areal density is 10^{10} cm^{-2}, and doping is 4×10^{10} cm^{-2} (4 electrons per QD).

The simulated QD structure consisted of 5 interchanging layers with QD clusters and layers of GaAs which were intentionally doped. Fig. 2 shows both three-dimensional potential profile as well as its cross-section in the middle of QD cluster shown by the dashed line. Dark area represent higher potential barriers whereas lighter area - low potential values. It is seen from Fig. 2 that in the area, which is outside of the QD cluster, the electron potential energy is about 10 meV, whereas around QDs it is about 110 meV slightly varying between QDs. Thus, in the area that is far from the QD cluster electrons can freely move laterally as well as in the perpendicular to the QD cluster layer direction. The characteristic picture of the QD cluster potential profile was obtained as it is seen

from Fig. 2 for the QD areal density equal to 10^{10} cm^{-2}. The doping of the GaAs layer adjacent to the layer with QD clusters is equal to 4×10^{10} cm^{-2}, thus resulting in ~4 electrons per each QD.

The photoelectron lifetime, i.e. the photocarrier capture time in QD structures, is a critical parameter of QDIP. The limiting values of the noise equivalent power, NEP, and detectivity, D^*, are determined by the generation - recombination noise, which is controlled by the capture processes [3],

$$NEP = \frac{h\nu}{\eta}\sqrt{\frac{2n_{th}V}{\tau_{cap}}}\ , \quad D^* \equiv \frac{\sqrt{S}}{NEP_{GR}} = \frac{\eta}{h\nu}\sqrt{\frac{\tau_{cap}}{2n_{th}d}}\ , \tag{1}$$

where η is the total quantum efficiency, n_{th} is the density of the thermally activated electrons in conducting states, V, S, and d are the sensor volume, area, and width, correspondingly. In weak electric fields, the capture rate, τ_{cap}^{-1}, may be calculated analytically. Calculations show that it depends exponentially on the value of the barrier height, V_m, [3]

$$\frac{1}{\tau_{capt}} = \frac{1}{\tau_0}\exp\left(-\frac{eV_m}{kT}\right), \tag{2}$$

where τ_0 is the capture time in the flat potential structure with the same geometrical parameters. The parameter τ_0 depends on the dot concentration, N_d, the characteristic dot size, a, with respect to the electron mean free path, ℓ, and positions of quantum dots.

According to Eq. 2, the capture time in the lateral structures exponentially increases with increasing of the dot concentration, dot's occupation, and the GaAs width 2*d*. In the VCDC structures, the capture time exponentially increases with increasing of the number of dots in a cluster and dot's occupation. Because of the logarithmic dependence of the potential barriers on the geometrical parameters, the capture time depends weakly on the cluster radius and average distance between dot clusters.

Analytical consideration of photoelectron kinetics is limited by small electric fields. To minimize the photoelectron transit time and to increase the photoconductive gain, QDIPs operate at significant biased voltages, which substantially change the photoelectron distribution functions. In the next section we consider kinetics in the lateral QD structures (Fig. 1.a) and VCDC structures (Fig. 1.b) on the basis of the Monte-Carlo modeling.

3. Photoelectron Kinetics in Strong Electric Fields

Our Monte-Carlo program includes all basic scattering mechanisms, such as electron scattering on acoustic, polar optical, and intervalley phonons. The program considers electrons which may populate Γ–, L–, and X– valleys and takes into account redistribution of carriers between valleys created by charged dots. We consider the carrier capture process as a specific inelastic scattering process, which is confined in space by the dot volume and in which a carrier is transferred from a conducting state above the potential barrier to a bound state below the barrier. We assume that from a bound state a carrier will relax to the deep dot states faster than it could return back to the conducting state.

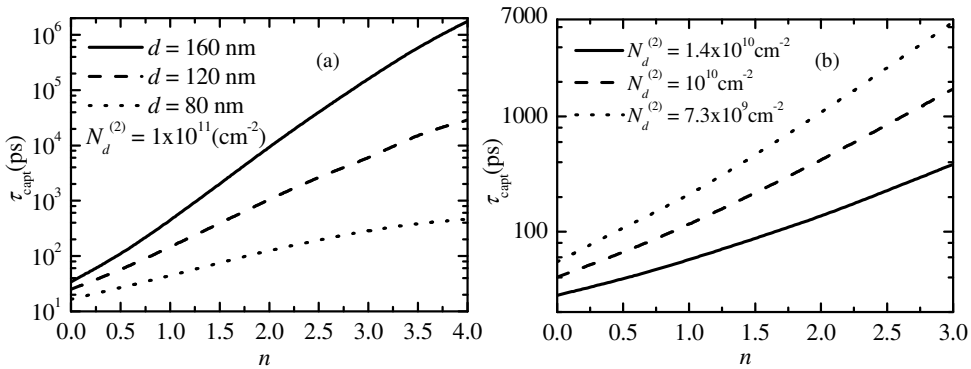

Fig. 3. Capture time as a function of potential barrier height, V_m, in QD structures (a) with lateral transport and (b) with VCDC and vertical transport.

Figure 3 presents the dependence of the capture time on the dot occupation, n, for both the lateral and VCDC structures. Parameters of the lateral structures are shown in the figure. For the VCDC structures we take the following parameters: $N = 9$, $b = 75$ nm, $c = 40$ nm, and the distance between the neighboring dots is 55 nm. As seen, the capture time has an exponential dependence on occupation, as it is expected from Eq. 2 taking into account that the barrier height depends linearly on the occupation.

Figure 4 shows the capture time as a function of the dot concentration. The dot concentration is an important factor to optimize the absorption of radiation by QD structures. Modern technologies can provide structures with dot concentration in the range of 10^9 - 10^{11} cm^{-2}. In the lateral structures, the potential barrier height increases linearly with increasing dot concentration. As seen this effect prevails at the dot occupation n = 2 and 3. At n =1, the effect has nonmonotonic character. At small dot concentations the barriers are small and by increasing the dot concentration we increase the number of traps for photoelectrons. Therefore, the capture time decreases with increasing the dot concentration. Charged dots form substantial potential barriers and the photoelectron time increases with increasing the dot concentration.

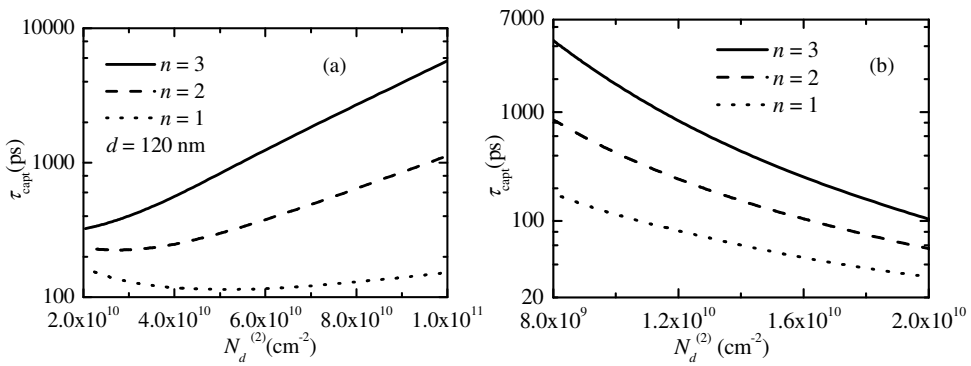

Fig. 4. Capture time as a function of dot concentration, $N_d^{(2)}$, in QD structures (a) with lateral transport and (b) with VCDC and vertical transport.

In VCDC structure, the dependence of capture time on dot concentration is opposite to that in the lateral structures (Fig. 4.b). In the VCDC structures, an increase of the dot concentration at fixed number of the dots per cluster leads to the decrease of the potential barriers. Besides this, it also results in an increase of traps for photoelectrons. For these reasons, capture time decreases with the increasing of the dot concentration.

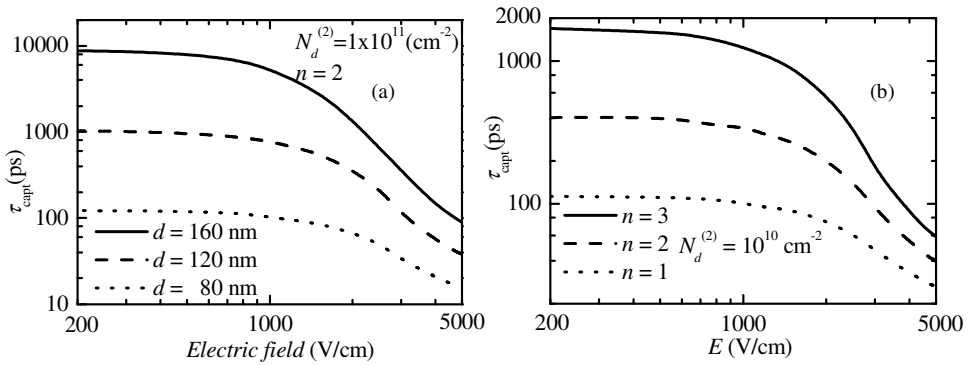

Fig. 5. Capture time as a function of electric field in QD structures (a) with lateral transport and (b) with VCDC and vertical transport.

Figure 5 shows the capture time as a function of electric field for the lateral and VCDC structures. At small electric field, the capture time changes just slightly and remains almost constant up to a characteristic value of electric field, ~ 1000 V/cm. Further increase in the electric field leads to substantial enhancement of the capture processes.

To understand the effects of the electric field on the capture time, we calculated the dependence of the average electron energy $\bar{\varepsilon}$ on the electric field (Fig. 6). Let us note that the average electron energy may be also evaluated from the energy balance equation, if one assumes that the nonequilibrium electron distribution function is described by

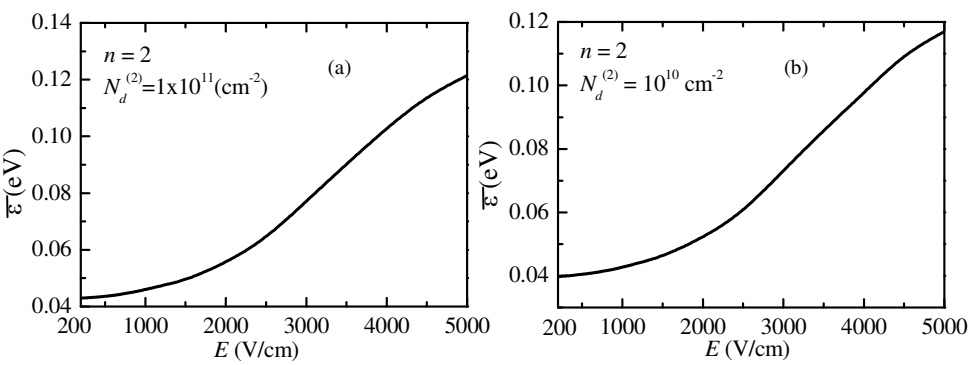

Fig. 6. Average electron energy as a function of the electric field in QD structures (a) with lateral transport and (b) with VCDC and vertical transport.

electron temperature. Both numerical and analytical calculations provide consistent results. Note, that in this range of field, the potential barriers don't change this dependence.

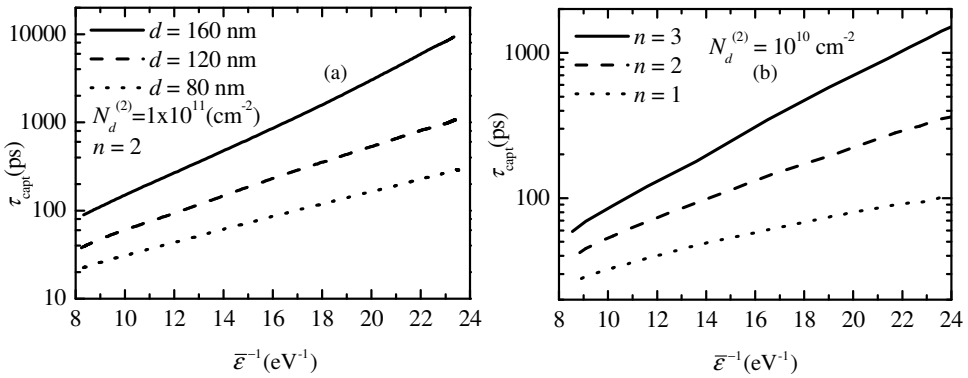

Fig. 7. Capture time as a function of the inverse electron energy attained in the electric field in QD structures (a) with lateral transport and (b) with VCDC and vertical transport.

Figure 7 presents the dependence of the capture time on the inverse value of $\overline{\varepsilon}$. As it is seen, log τ_{capt} is proportional to $1/\overline{\varepsilon}$, i.e. τ_{capt} is proportional to $\exp(1/\overline{\varepsilon})$. Thus, the carrier capture in the electric field can be described by Eq. 2, where the thermal energy kT is replaced by a factor of $\sim 2\overline{\varepsilon}/3$. Thus, we may conclude that the effect of the electric field on carrier capture is well described by the model of electron heating.

Finally, we calculated the photoconductive gain, g, as a function of the electric field for devices with the length of 1 μm. Photoconductive gain is defined as the ratio of the carrier lifetime, τ_{cap}, to carrier transit time, τ_{tr}. The photoelectron transit time is the time that the electron spends in the device moving from the emitter to the collector and, therefore, τ_{tr} is inversely proportional to the drift velocity. The average drift velocities have been calculated using the same Monte Carlo program. As seen from Fig. 8, the gain

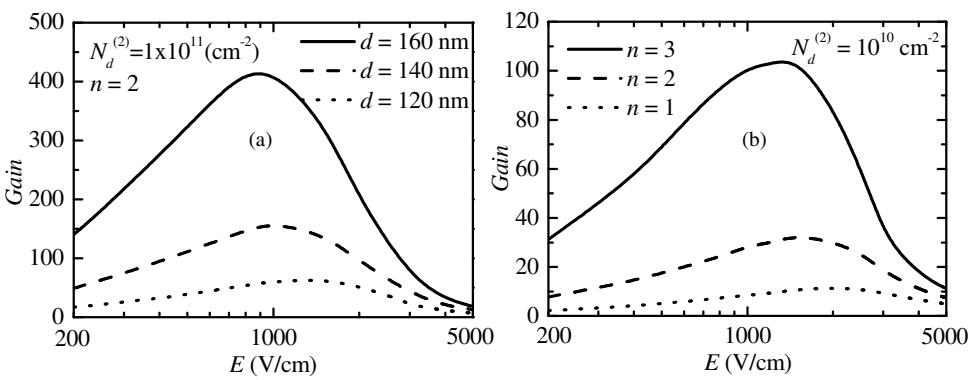

Fig. 8. Photoconductive gain as a function of electric field in QD structures (a) with lateral transport and (b) with VCDC and vertical transport. Length of both devices is 1 μm.

approaches a maximum value at electric field of the order of 10^3 V/cm, which is also the characteristic field for the dependences shown in Fig. 5. This nonmonotonic dependence on the electric field may be explained in the following way. At small electric fields, the gain increases with increasing of the electric field, since the transit time reduces and capture time remains almost constant. When the electric field increases up to a characteristic value, transit time almost saturates and capture time reduces substantially and, therefore, the gain decreases substantially.

In summary, photodetectors based on quantum dot structures with specially engineered potential barriers have a strong potential to overcome limitations of quantum-well-based devices for IR imaging. Such structures have a number of characteristics making them especially suitable for optoelectronic applications: (i) Manageable photoelectron kinetics; (ii) High photoconductive gain and responsivity; (iii) Low generation-recombination (GR) noise due to low concentration of thermo-excited carriers; (iv) High scalability of nanoblocks and numerous possibilities for nano-engineering; (v) Available fabrication technologies.

Here we presented the modeling of the photoelectron kinetics in the lateral structures and structures with vertically correlated dot clusters. Our results show that collective potential barriers around the groups of QDs effectively prevent photoelectron capture into the dots, while electric field overheats photoelectrons and enhances capture processes. Interplay of these two factors determines the optimal operating regime for QDIPs with potential barriers.

Acknowledgements

The research was supported by AFOSR (Mitin and Sergeev) and NSF under Grant No DMR 0907126 (Chien).

References

1. E. A. Zibik, T. Grange, B. A. Carpenter, N. E. Porter, R. Ferreira, G. Bastard, D. Stehr, S. Winnerl, M. Helm, H. Y. Liu, M. S. Skolnick, and L. R. Wilson, *Nature Materials* **8**, 403 (2009).
2. M. Razeghi, H. Lim, S. Tsao, J. Szafraniec, W. Zhang, K. Mi, and B. Movaghar, *Nanotechnology* **16**, 219 (2005).
3. J. C. Campbell and A. Madhukar, *IEEE Quantum Electronics* **95**, 1815 (2007).
4. A. V. Barve, S. J. Lee, S. K. Noh, and S. Krishna, *Laser & Photonics Reviews*, June 17 (2009).
5. M. D. Kelzenberg, D. B. Turner-Evans, B. M. Kayes, M. A. Filler, M. C. Putnam, N. S. Lewis, H. A. Atwater et al., *NANO Letters* **8**, 710 (2008).
6. H. Spanggaard and F. C. Krebs, *Solar Energy Materials and Solar Cells* **83**, 125 (2004).
7. U. Bockelmann and G. Bastard, *Phys. Rev. B* **42**, 8947 (1990).
8. Y. Toda, O. Moriwaki, M. Nishioka, and Y. Arakawa, *Phys. Rev. Lett.* **82**, 4114 (1999).
9. R. Ferreira and G. Bastard, *Appl. Phys. Lett.* **74**, 2818 (1999).
10. H. Lim, B. Movaghar, S. Tsao, M. Taguchi, W. Zhang, A. A. Quivy, and M. Razeghi, *Phys. Rev. B* **74**, 205321 (2006).
11. A. Sergeev, V. Mitin, and M. Stroscio, *Physica B* **316-317**, 369-372 (2002).
12. V. Mitin, N. Vagidov, and A. Sergeev, *Physica Status Solidi (C)* **3**, 4013-4016 (2006).

13. V. Mitin, A. Sergeev, L. H. Chien, and N. Vagidov, *Proceed. of SPIE: Nanophotonics and Macrophotonics for Space Environment II*, **7095**, 70950K1 - 70950K9 (2008).
14. L.-H. Chien, A. Sergeev, N. Vagidov, and V. Mitin, *Int. J. of High Speed Electronics and Systems* **18**, 1013-1022 (2008).
15. N. Vagidov, A. Sergeev, and V. Mitin, *Physics and Modeling of Tera- and Nano-Devices*, editors M. Ryzhii and V. Ryzhii, World Scientific, 141-148 (2008).
16. L. H. Chien, A. Sergeev, V. Mitin, and S. Oktyabrsky, *Proceed. of SPIE: SPIE Photonics West, Connecting Minds for Global Solutions* (2010), will be published.
17. http://www.nextnano.de/nextnano3/